

Description and Results of a Two-Dimensional Lattice Physics Code Benchmark for the Canadian Pressure Tube Supercritical Water-cooled Reactor (PT-SCWR)

D. W. Hummel, S. E. Langton, M. R. Ball, D. R. Novog and A. Buijs

McMaster University, Ontario, Canada

hummeld@mcmaster.ca

Abstract

Discrepancies have been observed among a number of recent reactor physics studies in support of the PT-SCWR pre-conceptual design, including differences in lattice-level predictions of infinite neutron multiplication factor, coolant void reactivity, and radial power profile. As a first step to resolving these discrepancies, a lattice-level benchmark problem was designed based on the 78-element plutonium-thorium PT-SCWR fuel design under a set of prescribed local conditions. This benchmark problem was modeled with a suite of both deterministic and Monte Carlo neutron transport codes. The results of these models are presented here as the basis of a code-to-code comparison.

1. Introduction

Atomic Energy of Canada Limited (AECL), in collaboration with Natural Resources Canada (NRCan) and the National Sciences and Engineering Research Council (NSERC), has developed a pre-conceptual SuperCritical Water-cooled Reactor (SCWR) design that is an evolution from more conventional Pressurized Heavy Water Reactors (PHWR), utilizing both pressure tubes and a low temperature heavy water moderator. This Pressure Tube type SCWR (PT-SCWR), unlike a typical PHWR, features batch refuelling, vertical fuel channels and light water coolant. The thermal isolation between the supercritical coolant and the low temperature and pressure moderator is provided by a porous ceramic insulator, eschewing the need for a separate calandria tube [1].

A reference fuel design for the PT-SCWR is the 78-element bundle shown in Figure 1, containing small diameter pins in the outermost ring and a large unfuelled centre pin. The fuel consists of a homogeneous mixture of 13 weight per cent PuO₂ in ThO₂. The reactor core consists of 336 channels, each containing a 5 m active length of fuel, with a channel lattice spacing of 25 cm. It is fuelled with a three-cycle batch refuelling scheme [2].

Recent independently performed reactor physics studies on this reference PT-SCWR cell have shown discrepancies in predictions of several lattice quantities, including the infinite lattice multiplication factor (k_{∞}), coefficient of Coolant Void Reactivity (CVR), and radial power profile including peak Linear Element Ratings (LERs). These studies were performed using a variety of different neutron transport codes, including both deterministic and Monte Carlo solution methods [3,4,5,6]. Since these lattice parameters have a significant impact on the PT-SCWR conceptual physics design, it was decided that a lattice physics benchmark problem was necessary in order to understand the sources and significance of these discrepancies [7].

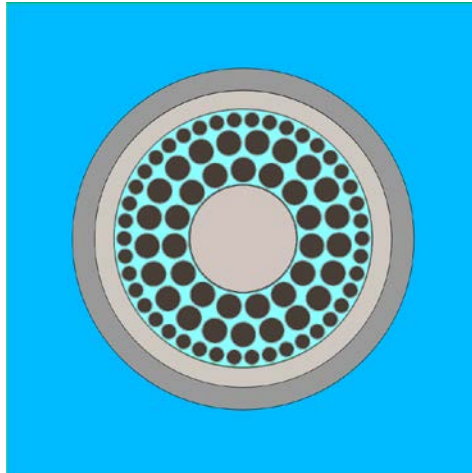


Figure 1 Reference 78-element PT-SCWR fuel design

2. Benchmark Problem Specification

The full benchmark description is provided in [7], and is freely available from the authors upon request. A brief description of the benchmark problem is nonetheless provided here to provide context for the presented results and analysis.

The geometry and material specification for the benchmark are for the most part identical to those presented in [3] for the 78-element PT-SCWR fuel design, with two notable exceptions. First, yttrium is not present in the freely available WIMSD format nuclear data libraries used by several of the computer codes in this benchmark, and so the yttrium is omitted in the centre pin and ceramic insulator [8]. Second, in [3] it is stated that the stainless steel liner tube is perforated and the ceramic insulator is porous, allowing the ingress of coolant into both. In the interest of model simplicity, for this benchmark no coolant ingress is allowed. For these reasons the code results presented in this work should not be considered truly representative of the reference fuel design in [3], but nonetheless provide a basis for code-to-code comparison.

To account for the large axial coolant density variation that is expected in the PT-SCWR channel at Hot Full Power (HFP) conditions, the lattice cell is specified at the five equally spaced locations shown in Table 1. Temperatures are only specified as 600 K and 900 K to accommodate the data available in the nuclear data libraries used by some of the codes in the benchmark, and avoid interpolation therein. Table 2 shows all other material temperatures, with only the centre pin and liner tube temperatures varying with axial position.

Fresh fuel composition is specified as the same 13 weight per cent PuO_2 in ThO_2 as is shown in [3]. An “exit burnup” isotopic composition at approximately $40 \text{ MW}\cdot\text{d}\cdot\text{kg}^{-1}$ was also specified based on calculations performed in WIMS-AECL, which varied by ring of fuel elements [7,9]. Both fresh and exit compositions were homogeneous along the axial length of the channel.

Table 1 Coolant Density and Temperature for Benchmark Problem [7]

Distance from Channel Inlet (m)	Coolant Density (kg·m ⁻³)	Coolant Temperature (K)
0.5	592.54	600
1.5	382.46	600
2.5	160.92	600
3.5	89.49	900
4.5	69.63	900

Table 2 Other Material Temperatures [7]

Material	Temperature (K)
Centre pin	Same as coolant
Fuel	900
Cladding	900
Liner tube	Same as coolant
Ceramic insulator	600
Pressure tube	600
Moderator	300

The lattice cells are evaluated under three different operating conditions. The first is the aforementioned Hot Full Power (HFP) condition with the temperatures specified as above. This is based on a core thermal power of 2,540 MW which, with 336 channels and a 5 m assembly containing 259 kg of fuel, corresponds to an average power density of 29.2 W·g⁻¹ of initial heavy elements [7]. The second operating condition is Cold Zero Power (CZP), where all material temperatures are 300 K and the coolant density is uniformly 996.567 kg·m⁻³. The third condition is Hot Zero Power (HZP), where all materials have a temperature of 600 K (save for the moderator which is always 300 K) and the coolant density remains 592.54 kg·m⁻³ at all axial positions. Note that in the CZP and HZP cases there is no axial variation in properties and thus only a single lattice cell model is required.

Two perturbation cases are additionally specified for each lattice cell model. The first is to calculate CVR, where the coolant density is changed to 1 kg·m⁻³ to represent “voided” conditions. The second perturbation case is to evaluate the Fuel Temperature reactivity Coefficient (FTC), where the fuel temperature in each lattice cell is increased by 100 K.

Altogether, including both fresh and exit burnup fuel, at multiple axial locations (if relevant), at three different operating conditions and two perturbations from these conditions, the benchmark problem requires 42 separate lattice calculations. The desired output from each of these calculations includes the value of k_{∞} , the value of CVR, the value of the FTC, and the radial power distribution.

3. Codes Used for the Benchmark Study

Multiple result submissions were received using a variety of different computer codes and nuclear data libraries. A brief description of each submission, including any relevant modelling features, is presented here.

3.1 DRAGON 3.06

DRAGON is a freely available code developed at École Polytechnique de Montréal that is capable of solving the neutron transport equation in both two and three dimensions using the collision probability method [11]. Three submissions were received using DRAGON. The first two share the same spatial meshing using DRAGON version 3.06K, executed with both the IAEA 172 group data library (henceforth specified as DRAGON 3.06K IAEA) and the ENDF/B-VII.0 172 group data library (DRAGON 3.06K ENDF/B-VII.0), both in WIMSD format as provided by the International Atomic Energy Agency Nuclear Data Service [8]. The third submission was developed independently from the others, with different spatial meshing and integration parameters, using DRAGON version 3.06H with the same ENDF/B-VII.0 172 group library (DRAGON 3.06H ENDF/B-VII.0).

3.2 WIMS-AECL 3.1

WIMS-AECL is a two-dimensional multigroup neutron transport code derived from the original WIMS code by Atomic Energy of Canada Limited (AECL[®]) and maintained by the Reactor and Radiation Physics Branch at Chalk River Laboratories. The submission to the benchmark was obtained using WIMS-AECL version 3.1.2.1 and an 89-group data library based on ENDF/B-VII.0 [9,11].

3.3 MCNP5

MCNP (Monte Carlo N-Particle) is a general purpose code developed by the Los Alamos National Laboratory that solves the neutron transport equation in continuous energy using the Monte Carlo method [12]. The submission for this benchmark used MCNP5 version 1.40 and nuclear data based on ENDF/B-VII.0 [11]. MCNP is widely used as a physics benchmarking tool due to the accuracy of its solution in continuous energy, and thus several results in this benchmark study are also reported relative to the corresponding MCNP value.

3.4 KENO

KENO solves the neutron transport equation using the Monte Carlo method and is part of the Standardized Computer Analysis for Licensing Evaluation (SCALE) code package developed by Oak Ridge National Laboratories [14]. Two submissions were received using KENO (versions V.a and VI), one using the 238-group ENDF/B-VII.0 nuclear data library and one using ENDF/B-VII.0 in continuous energy. In the case of the former, a self-shielding correction is necessary due to the multigroup nuclear data. This was performed using the MULTIREGION treatment in SCALE 6.1, requiring a 1-D approximation (annularization) of the lattice geometry over which the CENTRM/PMC module deterministically calculates a continuous energy neutron flux spectrum. This spectrum is used to correct the resonance absorption cross-sections for the Monte Carlo solution over the full geometry. The continuous energy KENO submission requires no self-shielding corrections, but only an incomplete set of results could be submitted.

4. Benchmark Results

Figure 2 and Figure 3 below show the simulation results for the infinite lattice multiplication factor (k_{∞}) as a function of position along the PT-SCWR channel under Hot Full Power conditions (or to be

more precise, as a function of coolant density and temperature according to the benchmark problem definition in Table 1 and Table 2).

It is seen that the bias between MCNP and the other codes is on the order of several mk, but most submissions predict the same general trend with changes in coolant density over the length of the entire channel. The variation in code predictions for fresh fuel is greatest where the coolant density is highest (near the channel inlet). Relatively speaking the variation between predictions for the depleted fuel composition is larger but the same general trends are still followed. The results obtained with DRAGON using the WIMSD format ENDF/B-VII.0 library are the greatest relative outliers, whereas DRAGON results obtained with the WIMSD format IAEA library (and in one case, the same spatial meshing) are closer to the middle of all code predictions.

Most noteworthy of these results is the fact that between the 0.5 m and 1.5 m locations different codes show different sensitivities with decreasing coolant density (all other lattice properties remaining constant). Some predict practically no change or a very small increase in k_{∞} , and the largest outliers show a *decrease* in k_{∞} on the order of one mk even though the general trend with decreasing coolant density is an increase in reactivity for this benchmark problem.

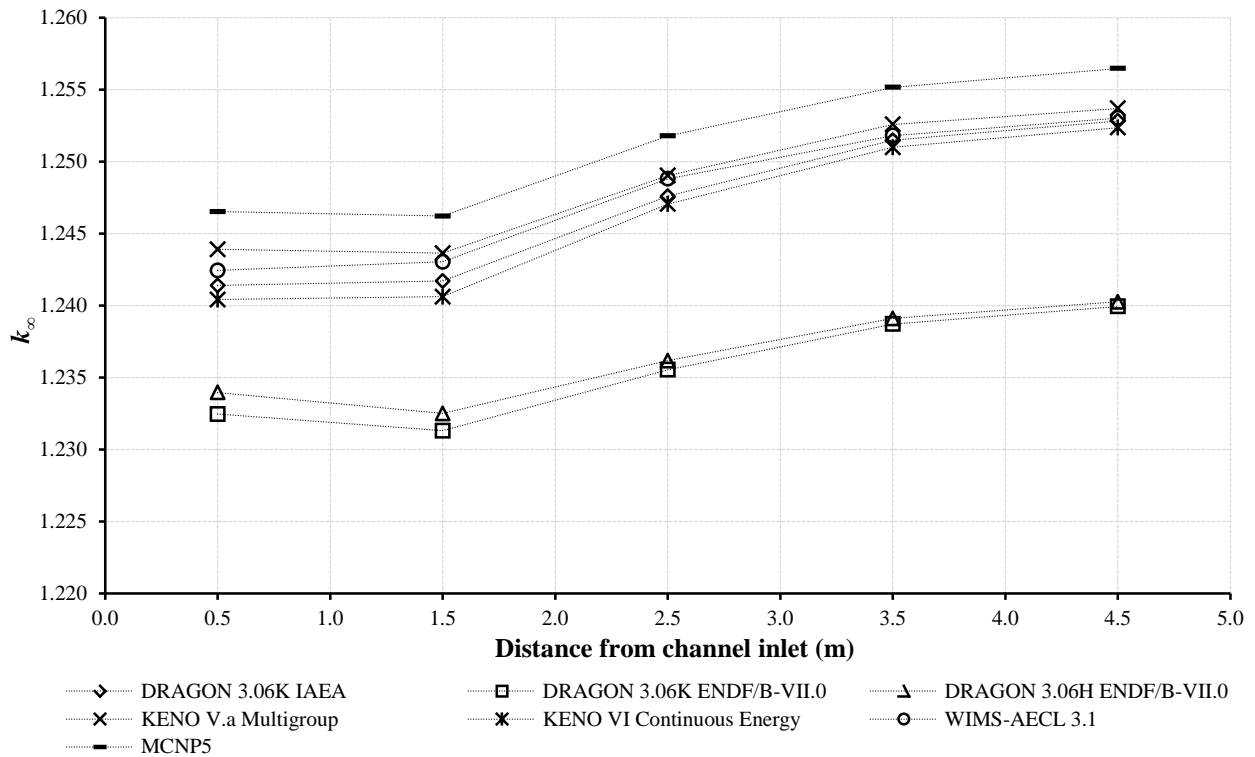


Figure 2 k_{∞} results for fresh fuel

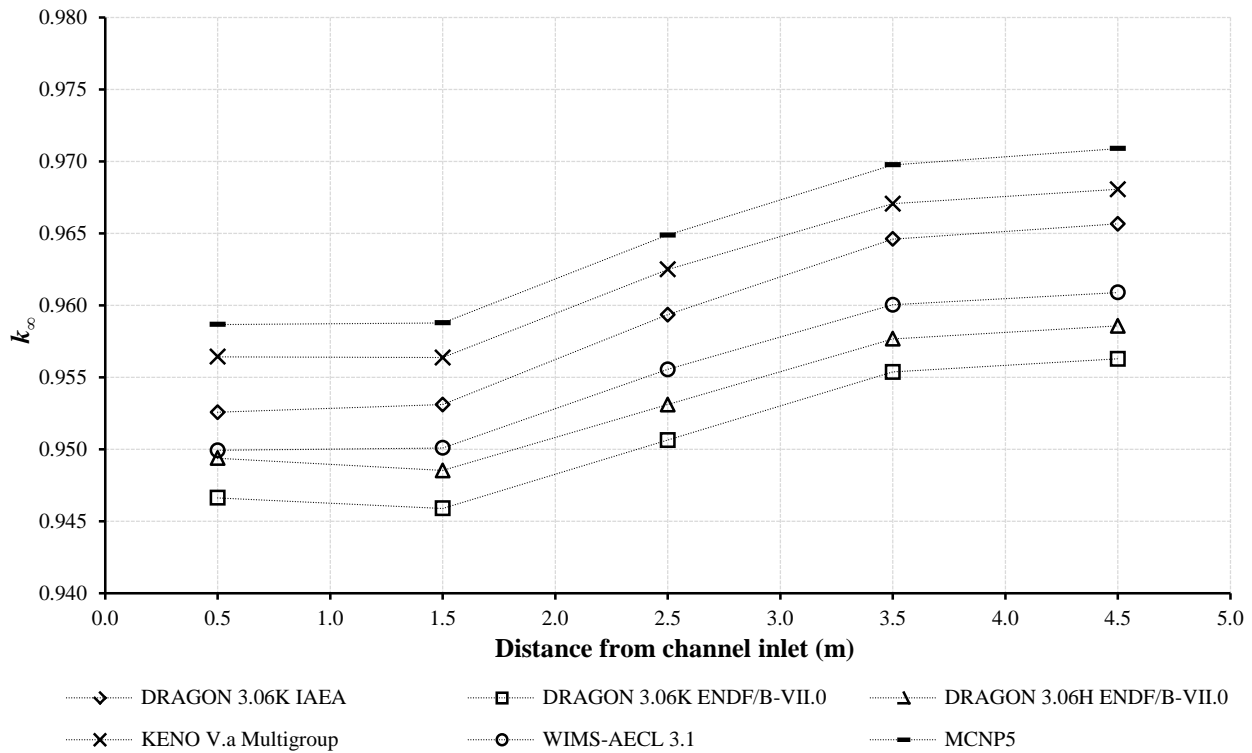


Figure 3 k_{∞} results for exit burnup fuel

The code results for CVR are shown in Figure 4 and Figure 5. In absolute terms the variation between code predictions is much higher near the channel inlet, however this not surprising because in absolute terms the change in coolant density for the “voided” case is also much larger according to Table 1, and a larger reactivity worth would be expected. Since the properties of the “voided” cell at each location are essentially the same (excluding the relatively small impact of non-fuel material temperatures), the variation in predictions of reactivity worth result mostly from the bias and variation in k_{∞} predictions discussed previously. Again, note that the code results show a different trend for decreasing coolant density between the 0.5 m and 1.5 m locations.

Figure 6 and Figure 7 show the code predictions for the FTC. In the fresh fuel case most code results show that the FTC is largely insensitive to the effects of changing coolant density along the length of the channel, with the exception of KENO (both in continuous energy and multigroup). With the exit burnup fuel composition the variation between code predictions is larger, and each code shows a greater sensitivity to coolant density.

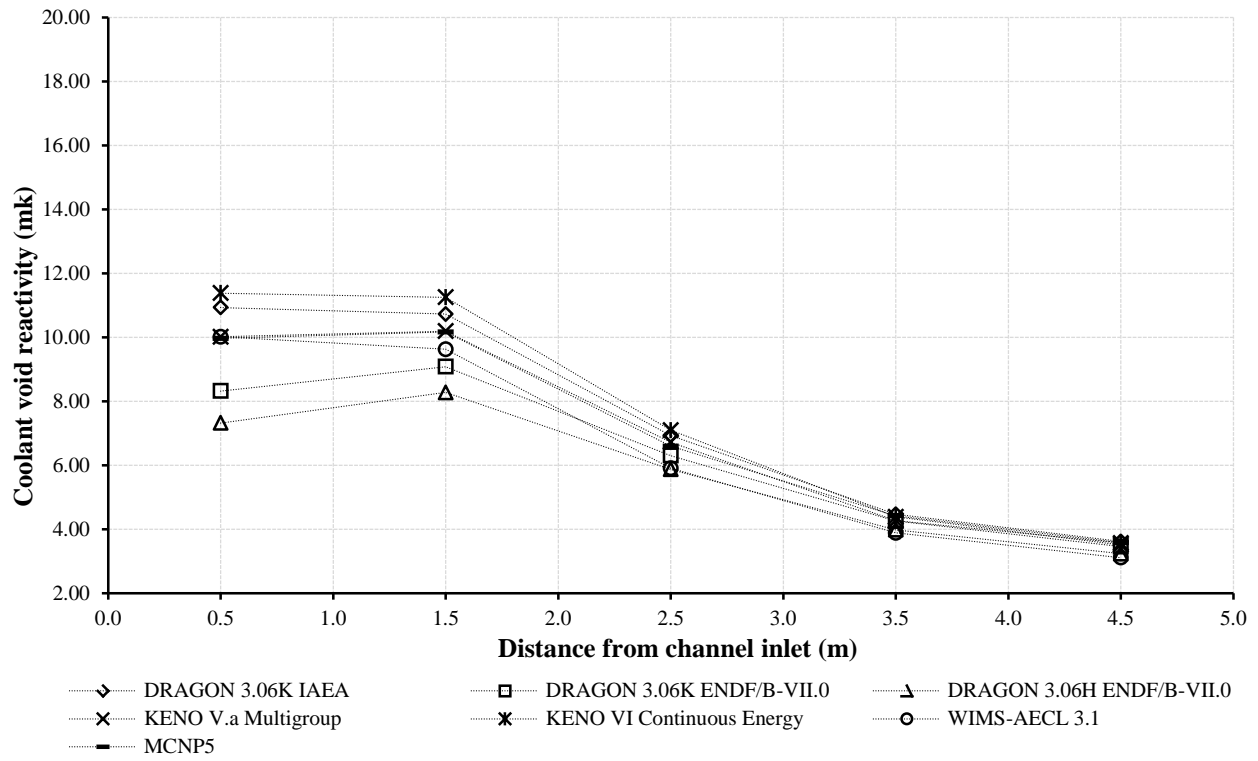


Figure 4 CVR results for fresh fuel

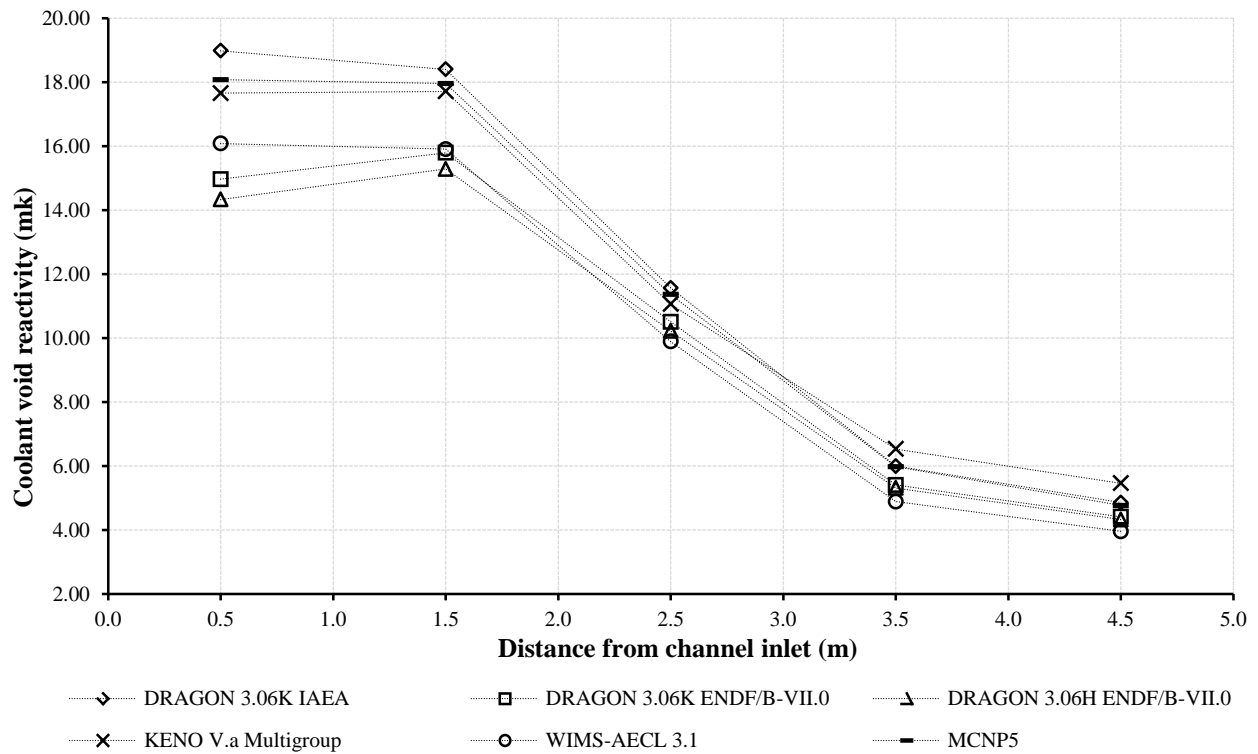


Figure 5 CVR results for exit burnup fuel

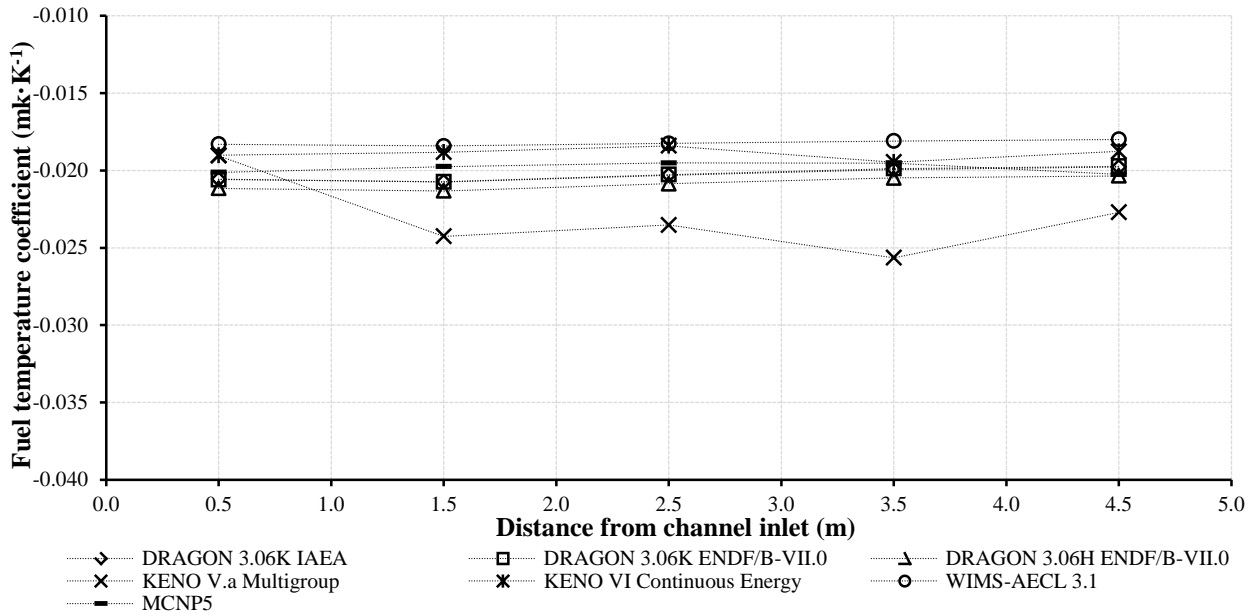


Figure 6 FTC results for fresh fuel

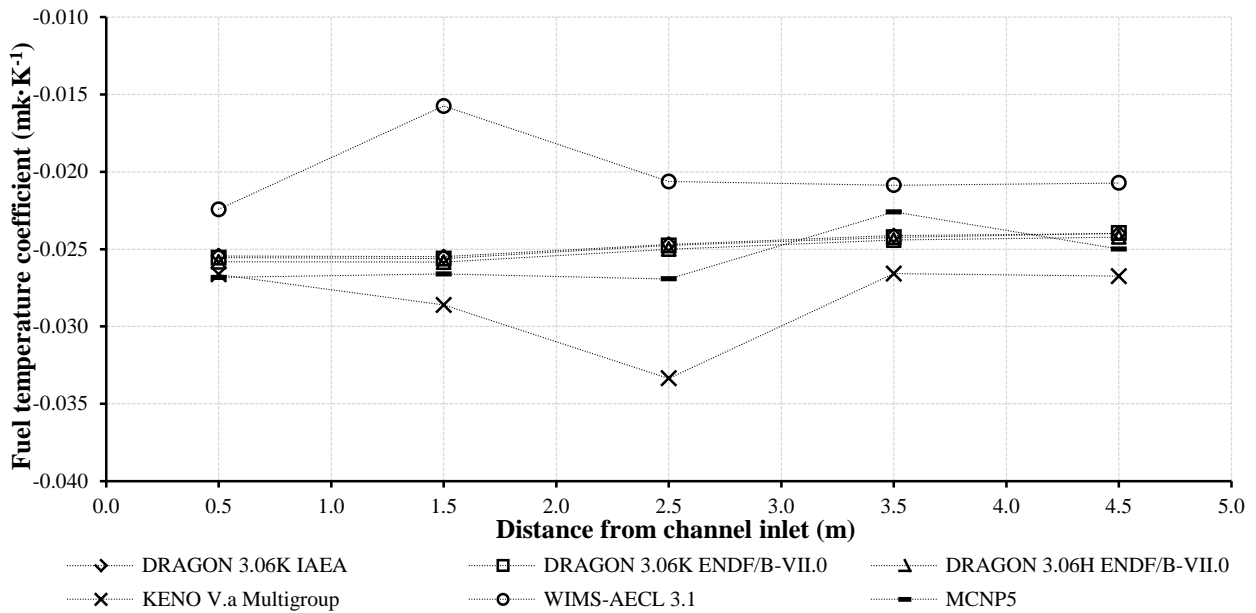


Figure 7 FTC results for exit burnup fuel

Figure 8 through Figure 13 show the LER at each axial position for a ring of fuel elements. Taken together these represent the radial power profile across the fuel assembly at each axial location. The span of each plot is kept the same to facilitate comparisons between code predictions, but note that the limits of each scale are not necessarily identical.

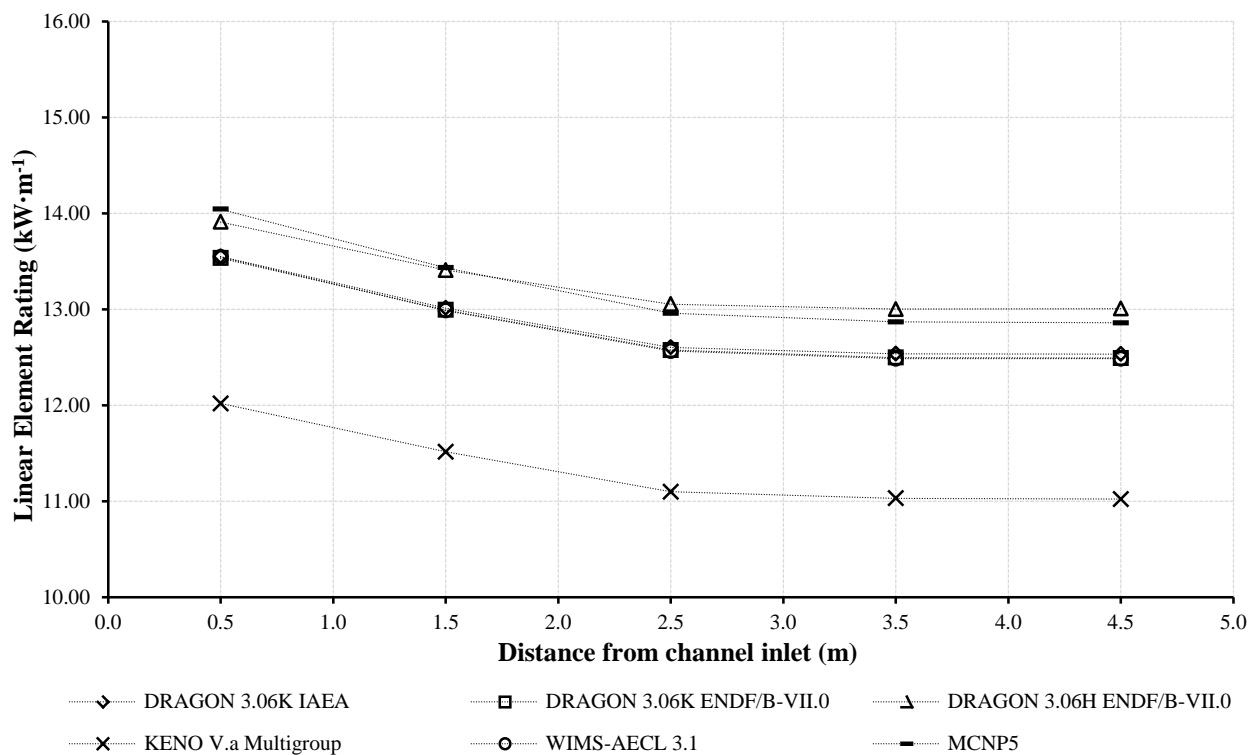


Figure 8 LER results for the innermost ring of elements with fresh fuel

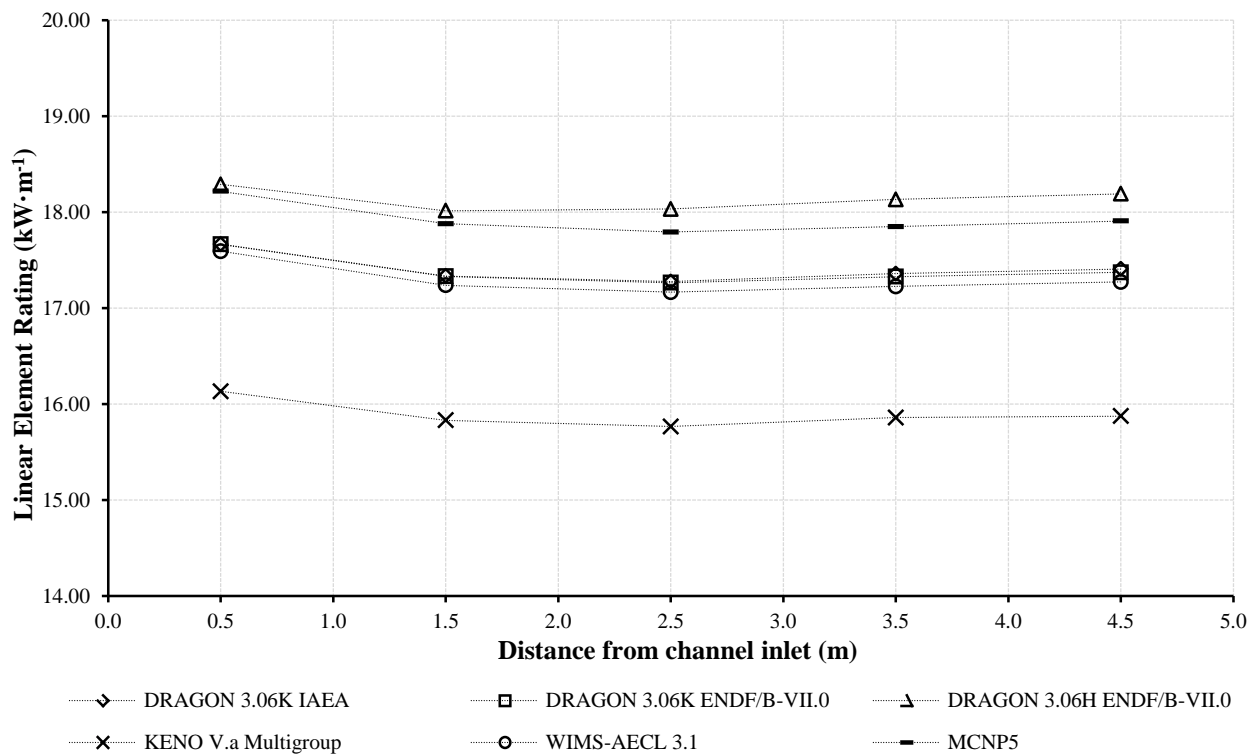


Figure 9 LER results for the innermost ring of elements with exit burnup fuel

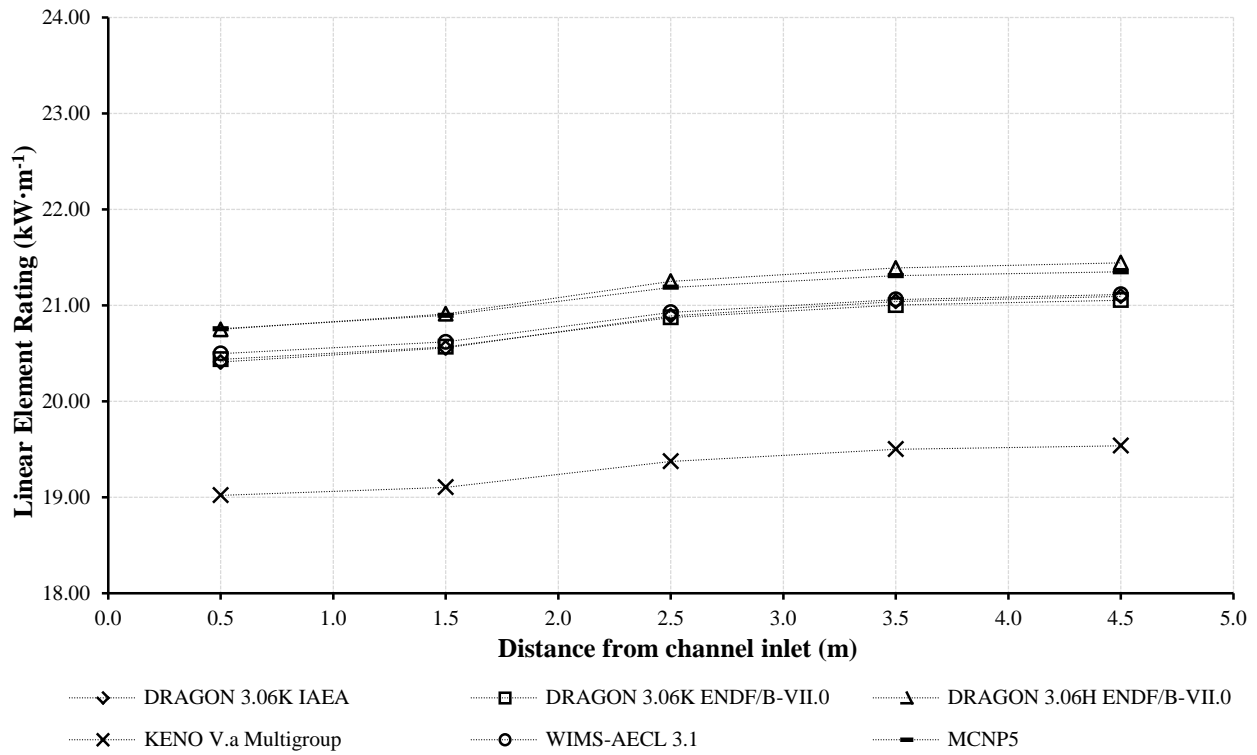


Figure 10 LER results for the middle ring of elements with fresh fuel

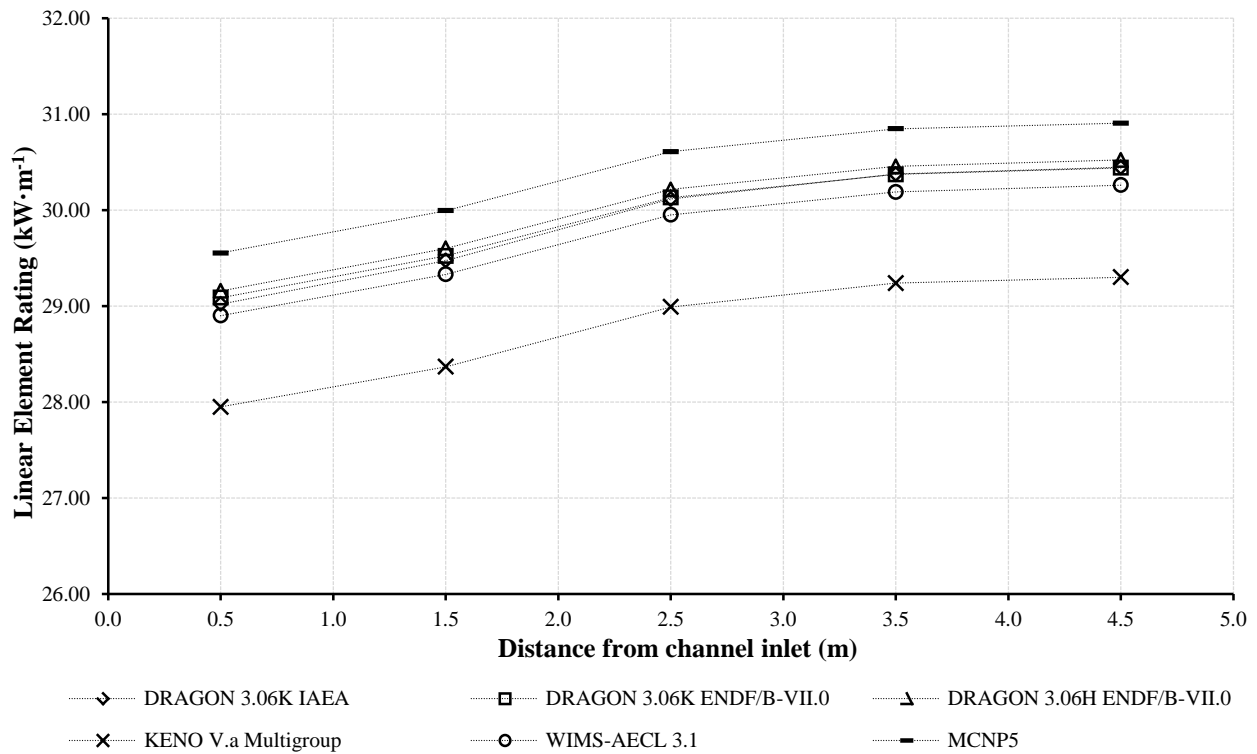


Figure 11 LER results for the middle ring of elements with exit burnup fuel

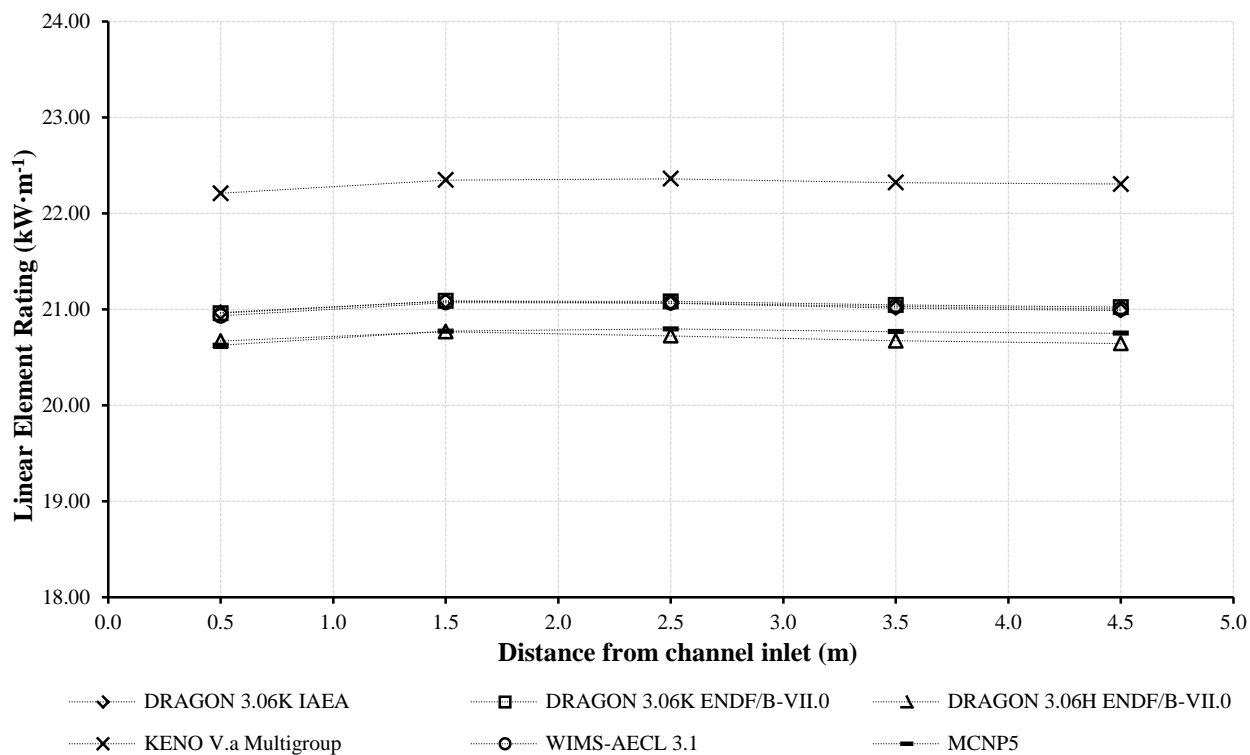


Figure 12 LER results for the outer ring of elements with fresh fuel

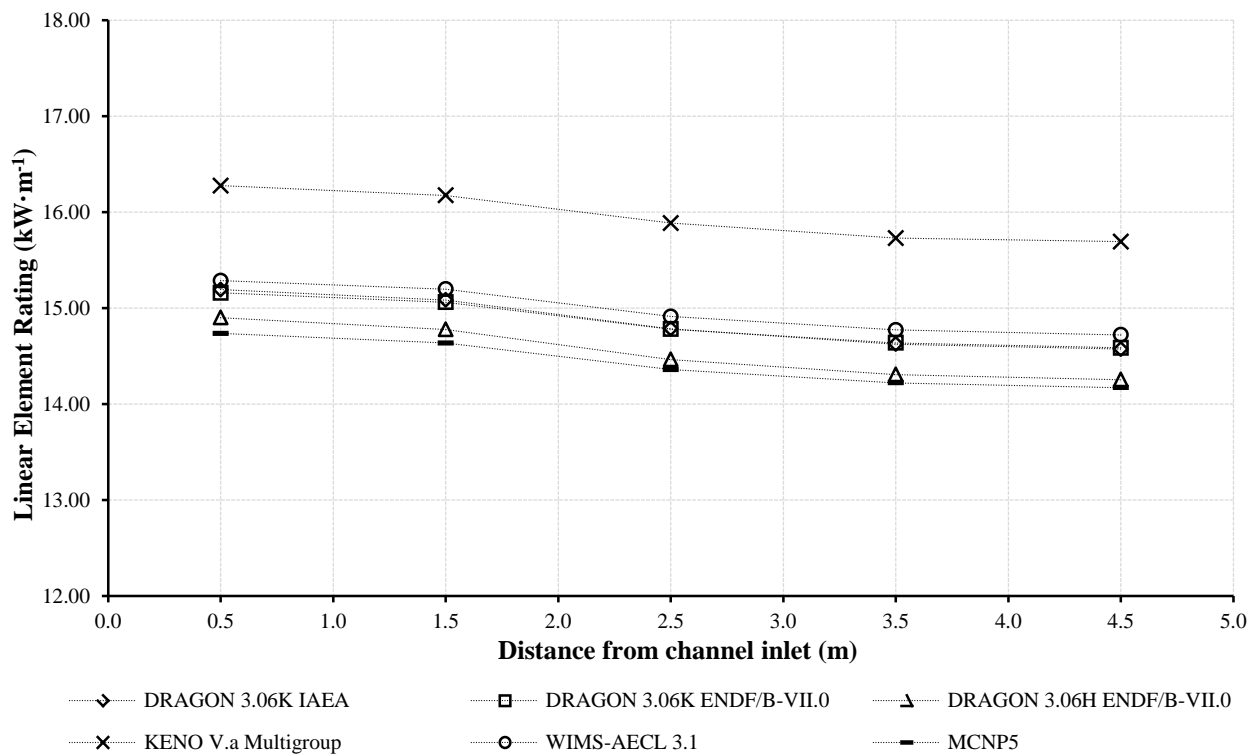


Figure 13 LER results for the outer ring of elements with exit burnup fuel

For these benchmark calculations the total bundle power is constrained to a single value, and thus if the LER prediction for a single ring of elements is relatively low then the LER for another ring must be relatively high to compensate. For fresh fuel it is seen that the results from DRAGON using the ENDF/B-VII.0 library closely mirror the MCNP results, while the other codes generally show lower LERs near the bundle interior and higher LERs in the outermost ring (i.e. a more outer-peaked radial power profile). With burnt fuel the variations in code predictions are not substantially different.

The LER predictions obtained from KENO in multigroup mode are substantial outliers from the other code predictions. It is possible that this results from the one-dimensionalization (annularization) necessary for the resonance self-shielding calculation when using KENO in multigroup mode. Other studies have shown that annularization may substantially affect the relative radial reaction rates in complex cluster geometries without having a substantial impact on the predicted integral properties of the lattice cell (e.g. k_{∞} or reactivity worth) [14]. Although annularization was only necessary for the resonance self-shielding component of the lattice calculation, it is otherwise difficult to reconcile the fact that the presented multigroup KENO results were not outliers for the other lattice parameters.

Table 3 through Table 6 show the calculation results for both the CZP and HZP conditions. Since each axial position is identical under these prescribed conditions only a single lattice calculation is necessary. To facilitate comparison between codes, each result's difference from the MCNP5 prediction is also provided.

Table 3 Collected Cold Zero Power (CZP) results for fresh fuel

	k_{∞}	$\Delta_{\text{MCNP}} k_{\infty}$ (mk)	CVR (mk)	$\Delta_{\text{MCNP}} \text{CVR}$ (mk)	FTC (mk·K ⁻¹)	$\Delta_{\text{MCNP}} \text{FTC}$ (mk·K ⁻¹)
DRAGON 3.06K (IAEA)	1.2710	-4.27	+8.16	+2.23	-0.0344	-0.0015
DRAGON 3.06K (ENDF/B-VII.0)	1.2647	-8.23	+3.84	-2.09	-0.0338	-0.0010
DRAGON 3.06H (ENDF/B-VII.0)	1.2676	-6.40	+2.51	-3.42	-0.0348	-0.0019
KENO V.a Multigroup	1.2771	-0.56	+5.66	-0.27	-0.0428	-0.0100
KENO VI Continuous Energy	1.2711	-4.24	N/A	N/A	N/A	N/A
WIMS-AECL 3.1	1.2685	-5.84	+8.02	+2.09	-0.0286	+0.0043
MCNP5	1.2780		+5.93		-0.0328	

Table 4 Collected Cold Zero Power (CZP) results for exit burnup fuel

	k_{∞}	$\Delta_{\text{MCNP}} k_{\infty}$ (mk)	CVR (mk)	$\Delta_{\text{MCNP}} \text{CVR}$ (mk)	FTC (mk·K ⁻¹)	$\Delta_{\text{MCNP}} \text{FTC}$ (mk·K ⁻¹)
DRAGON 3.06K (IAEA)	0.9650	-7.86	+23.75	+1.66	-0.0436	-0.0002
DRAGON 3.06K (ENDF/B-VII.0)	0.9611	-12.10	+17.61	-4.48	-0.0432	+0.0002
DRAGON 3.06H (ENDF/B-VII.0)	0.9647	-8.23	+16.44	-5.64	-0.0436	-0.0002
KENO V.a Multigroup	0.9713	-1.16	+21.96	-0.12	-0.0490	-0.0056
WIMS-AECL 3.1	0.9598	-13.55	+21.44	-0.65	-0.0333	+0.0101

MCNP5	0.9724		+22.08		-0.0434	
-------	--------	--	--------	--	---------	--

Table 5 Collected Hot Zero Power (HZP) results for fresh fuel

	k_{∞}	$\Delta_{\text{MCNP}} k_{\infty}$ (mk)	CVR (mk)	$\Delta_{\text{MCNP}} \text{CVR}$ (mk)	FTC (mk·K ⁻¹)	$\Delta_{\text{MCNP}} \text{FTC}$ (mk·K ⁻¹)
DRAGON 3.06K (IAEA)	1.2521	-3.30	+10.56	+1.21	-0.0240	+0.0008
DRAGON 3.06K (ENDF/B-VII.0)	1.2435	-8.81	+7.94	-1.41	-0.0251	-0.0004
DRAGON 3.06H (ENDF/B-VII.0)	1.2453	-7.62	+6.96	-2.39	-0.0259	-0.0011
KENO V.a Multigroup	1.2554	-1.21	+9.03	-0.32	-0.0290	-0.0042
KENO VI Continuous Energy	1.2515	-3.66	N/A	N/A	N/A	N/A
WIMS-AECL 3.1	1.2520	-3.33	+10.03	+0.68	-0.0221	+0.0026
MCNP5	1.2573		+9.35		-0.0247	

Table 6 Collected Hot Zero Power (HZP) results for exit burnup fuel

	k_{∞}	$\Delta_{\text{MCNP}} k_{\infty}$ (mk)	CVR (mk)	$\Delta_{\text{MCNP}} \text{CVR}$ (mk)	FTC (mk·K ⁻¹)	$\Delta_{\text{MCNP}} \text{FTC}$ (mk·K ⁻¹)
DRAGON 3.06K (IAEA)	0.9603	-6.69	+18.29	+1.05	-0.0300	+0.0005
DRAGON 3.06K (ENDF/B-VII.0)	0.9546	-12.88	+14.29	-2.94	-0.0313	-0.0008
DRAGON 3.06H (ENDF/B-VII.0)	0.9575	-9.73	+13.66	-3.58	-0.0315	-0.0010
KENO V.a Multigroup	0.9649	-1.69	+17.18	-0.06	-0.0351	-0.0046
WIMS-AECL 3.1	0.9563	-10.99	+16.12	-1.12	-0.0255	+0.0050
MCNP5	0.9665		+17.23		-0.0305	

The same trends between code predictions that were observed for the HFP case generally hold for both the CZP and HZP cases as well, with the single exception of the WIMS-AECL CVR predictions with fresh fuel. Observe in Figure 4 that WIMS-AECL always predicts a *lower* CVR value than MCNP5 for fresh fuel regardless of axial position, but for both the CZP and HZP conditions with fresh fuel WIMS-AECL predicts a *higher* CVR value. The other code predictions maintain their bias between MCNP5 and one-another at HFP.

5. Conclusions

A number of important conclusions can be made based on the presented code results and observations:

1. The effect of the nuclear data library on the DRAGON results is larger than the effect of the spatial meshing, assuming both spatial meshes were sufficiently descriptive of the geometry. The DRAGON results obtained with the WIMSD format ENDF/B-VII.0 library have a much larger bias in k_{∞} from MCNP5 than the other code results, including the DRAGON model using the WIMSD format IAEA library.

2. While the codes predict the same general trends with decreasing coolant density along the length of the entire PT-SCWR channel, this is not the case for relatively smaller (although still greater than $200 \text{ kg}\cdot\text{m}^{-3}$) coolant density change between 0.5 m and 1.5 m from the channel inlet. Between these locations different codes may predict an increase, decrease, or essentially no change in some lattice properties. The most significant impact of these differences is on the CVR value, which may vary by as much as 5 mk.
3. Code predictions generally vary more substantially for the exit burnup fuel composition than fresh fuel. In the case of burnt fuel, a much larger number of different isotopes are present, including both fission products and actinides which, depending on their concentrations, make any inconsistencies between different nuclear data libraries more evident. If the different codes used in this benchmark study were required to evaluate their own exit burnup composition (where capable) as opposed to being given one, the differences between the presented code results would likely be much larger.
4. Different codes may predict slightly different radial power profiles in the fuel assembly (either slightly flatter or more outer-peaked), but the effect on the LERs is typically limited to a variation of less than $1 \text{ kW}\cdot\text{m}^{-1}$. Note that this benchmark problem used an axially flat power profile. If a more realistic axial power profile was used (i.e. peaked in some location along the channel) the absolute variation in LERs would likely be larger (if the same relative differences were maintained). Also it should be noted that the radial power profile predicted by KENO V.a in multigroup mode was a significant outlier from the other code results.

Although the benchmark problem specification allowed these differences between code predictions to be observed, there is insufficient information to conclude why these differences exist. For a “second phase” of this PT-SCWR physics study it is suggested that additional results be requested for each code submission. These should include energy dependent relative reaction rates, including absorption in the fuel and non-fuel regions, and potentially isotopic reaction rates if the differences between nuclear data libraries are to be explored. Also included could be few-group condensed fluxes in different regions, and possibly few-group homogenized properties for the entire lattice cell.

Acknowledgments

The authors would like to thank Natural Resources Canada (NRCan) and the National Sciences and Engineering Research Council (NSERC) for support of the Canadian Generation IV PT-SCWR research project, Dr. Guy Marleau from École Polytechnique de Montréal for his participation in defining the benchmark problem, and Jeremy Pencer and Laura Blomeley from AECL Chalk River for their participation in the benchmark study.

6. References

- [1] L. K. H. Leung et al. “A Next Generation Heavy Water Nuclear Reactor with Supercritical Water as Coolant,” in HWR-Future - International Conference on Future of Heavy Water Reactors, Ottawa, Canada 2011.

- [2] J. Pencer and B. Hyland, “Physics Aspects of the Pressure Tube Type SCWR Preconceptual Design,” in HWR-Future - International Conference on Future of Heavy Water Reactors, Ottawa, Canada 2011.
- [3] J. Pencer, M. Edwards and N. Onder, “Axial and Graded Enrichment Options for the Canadian SCWR,” in CCSC-2012 - The 3rd China-Canada Joint Workshop on Supercritical-Water-Cooled Reactors, Xi’an, China 2012.
- [4] D. W. Hummel and D. R. Novog, “Fuel Composition Optimization in a 78-Element Fuel Bundle for use in a Pressure Tube Type Supercritical Water-Cooled Reactor,” in CCSC-2012 - The 3rd China-Canada Joint Workshop on Supercritical-Water-Cooled Reactors, Xi’an, China 2012.
- [5] G. Harrison and G. Marleau, “Computation of a Canada SCWR Unit Cell with Deterministic and Monte Carlo Codes,” in PHYSOR 2012 - Advances in Reactor Physics, Knoxville, USA 2012.
- [6] S. E. Langton, A. Buijs, T. Zhu and D. R. Novog, “Monte Carlo Simulation of a Burnup-Averaged 78-Element Canadian SCWR and Similarity Study with the ZED-2 Test Reactor,” in CCSC-2012 - The 3rd China-Canada Joint Workshop on Supercritical-Water-Cooled Reactors, Xi’an, China 2012.
- [7] J. Pencer and L. Blomely, “A Preliminary SCWR 2D Lattice-Level Benchmark Comparison of WIMS-AECL and MCNP,” 217-123700-REPT-005, Atomic Energy of Canada Limited, Chalk River, Canada 2012.
- [8] International Atomic Energy Agency Nuclear Data Services, “WIMS Library Update Project,” Internet: <http://www-nds.iaea.org/wimsd/> Jan. 28, 2008 [Oct. 29, 2012].
- [9] D. Altiparmakov, “New Capabilities of the Lattice Code WIMS-AECL,” in PHYSOR 2008 – International Conference on the Physics of Nuclear Reactors, Nuclear Power: A Sustainable Resource, Interlaken, Switzerland 2008.
- [10] G. Marleau, A. Hébert and R. Roy, “A user guide for DRAGON 3.06,” École Polytechnique de Montréal, Montréal, Canada, Technical Report IGE-174 Rev. 7, 2008.
- [11] D. Altiparmakov, “ENDF/B-VII.0 Versus ENDF/B-VI.8 in CANDU Calculations,” in PHYSOR 2008 – International Conference on the Physics of Nuclear Reactors, Nuclear Power: A Sustainable Resource, Interlaken, Switzerland, 2008.
- [12] X-5 Monte Carlo Team, “MCNP – A General Monte Carlo N-Particle Transport Code, Version 5,” LA-UR-03-1987, Los Alamos National Laboratory, Los Alamos, 2003.
- [13] S. M. Bowman, “SCALE 6: Comprehensive Nuclear Safety Analysis Code System,” *Nuclear Technology*, vol. 174 no. 2, pp. 126-148, May 2011.
- [14] M. R. Ball, A. C. Morreale, D. R. Novog and J. C. Luxat, “The Effect on Super-Cell Calculations Due to Modelling CANDU Fuel Pin Clusters as Annuli” in International Conference on Mathematics and Computational Methods Applied to Nuclear Science and Engineering (M&C 2011), Rio de Janeiro, Brazil, 2011.